

# Efficient Catalytic System for Synthesis of *trans*-Stilbene from Diphenylacetylene Using Rh-Based Intermetallic Compounds

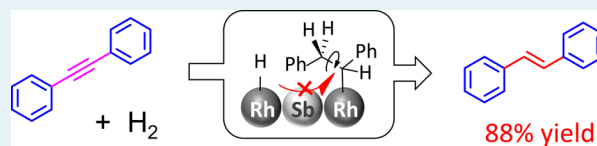
Shinya Furukawa,<sup>†</sup> Akira Yokoyama,<sup>‡</sup> and Takayuki Komatsu<sup>\*,‡</sup>

<sup>†</sup>Department of Chemistry and <sup>‡</sup>Department of Chemistry and Materials Science, Tokyo Institute of Technology, 2-12-1-E1-10 Ookayama, Meguro-ku, Tokyo 152-8551, Japan

## Supporting Information

**ABSTRACT:** A series of Rh-based intermetallic compounds supported on silica (Rh<sub>m</sub>M'<sub>n</sub>/SiO<sub>2</sub>, M' = Bi, Ge, In, Sb, and Sn) were prepared and tested as catalysts for *trans*-stilbene (*trans*-ST) synthesis from diphenylacetylene (DPA) in H<sub>2</sub> atmosphere. Rh<sub>2</sub>Sb/SiO<sub>2</sub> exhibited high catalytic activity in the semihydrogenation of DPA to *cis*-ST and subsequent isomerization to *trans*-ST, with a smaller capability of overhydrogenation to diphenylacetylene (DPE) than Rh/SiO<sub>2</sub>, affording a moderate yield of *trans*-ST (58%) after complete conversion of DPA. RhSb/SiO<sub>2</sub> possesses a unique hydrogenation property capable of half-hydrogenation but minimal overhydrogenation, which enables highly selective isomerization of *cis*-ST to *trans*-ST. A tandem catalytic system using RhSb/SiO<sub>2</sub> and Pd<sub>3</sub>Bi/SiO<sub>2</sub> afforded 88% yield of *trans*-ST. These results are the first examples of the effective synthesis of *trans*-ST from DPA using heterogeneous metallic catalysts.

**KEYWORDS:** *trans*-stilbene, diphenylacetylene, hydrogenation, isomerization, intermetallic compound

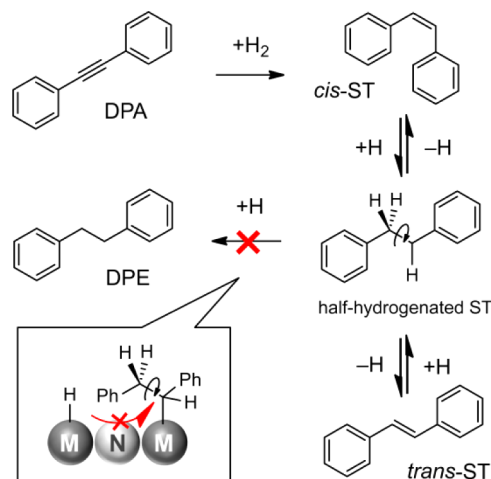


The compound *trans*-stilbene (*trans*-ST) is an important building block of useful materials such as dyes, fluorescent whitener,<sup>1</sup> liquid crystals,<sup>2</sup> and organic light-emitting diodes.<sup>3</sup> A common procedure for *trans*-ST synthesis employed to date has been the coupling of two aryl components by Wittig<sup>4</sup> or Heck-type reaction.<sup>5</sup> However, these methods require stoichiometric amounts of organic reagents such as a base. Therefore, the development of an atom-efficient heterogeneous catalytic system affording *trans*-ST with high yields is needed. In this context, semihydrogenation of diphenylacetylene (DPA) is a promising candidate for *trans*-ST synthesis. In general, semihydrogenation of alkyne to alkene is achieved over Pd-based bimetallic materials,<sup>6–11</sup> as represented by the Lindlar catalyst.<sup>6</sup> We have also reported that a Pd-based intermetallic compound, Pd<sub>3</sub>Bi, supported on SiO<sub>2</sub>, exhibited a high selectivity in the semihydrogenation of DPA.<sup>11</sup> In the case of inner alkene, however, *cis*- or (*Z*)-alkene is formed as a primary product.<sup>11,12</sup> To this day, only a few homogeneous catalysts have achieved the selective hydrogenation of alkynes to *trans*- or (*E*)-alkenes.<sup>13</sup> Therefore, the development of an efficient heterogeneous catalytic system for *trans*-ST synthesis from DPA remains a challenge. In this context, a potentially effective approach is to develop a catalyst capable of not only the semihydrogenation of DPA but also isomerization of *cis*-ST to *trans*-ST.

The *cis*–*trans* isomerization of alkene always requires the half breaking of a C=C bond into the corresponding single bond so that rotation along with the C–C axis is allowed. In the presence of hydrogen, addition of one hydrogen atom to the C=C bond moiety (half-hydrogenation) enables this bond breaking. A reverse reaction, that is, the elimination of the hydrogen with the C–C bond rotation, can afford a

thermodynamically stable *trans*-isomer (Scheme 1). However, it should be noted that overhydrogenation to alkane (diphenyl-

## Scheme 1. Reaction Pathways and Strategy for *trans*-ST Synthesis from DPA in the Presence of Hydrogen



ethane, DPE, for the case of DPA) must be inhibited. Therefore, it is an ideal approach to construct reaction sites capable of catalyzing the primary addition of a hydrogen atom but inhibiting the secondary addition.

Received: July 3, 2014

Revised: August 17, 2014

Published: September 9, 2014

In this study, we focused on intermetallic compounds as promising materials having such a specific hydrogenation ability. Intermetallic compounds often have active metal sites diluted or isolated by second metal atoms inert to hydrogenation and have specific atomic arrangements on their surface. Several unique hydrogenation properties of intermetallic compounds have been recently reported such as semihydrogenation of alkynes to alkenes ( $\text{Al}_{13}\text{Fe}_4$ ,<sup>14</sup>  $\text{NiGa}$ ,<sup>15</sup>  $\text{Pd}_3\text{Bi}$ ,<sup>11</sup>  $\text{PdGa}$ <sup>16</sup>), chemoselective hydrogenation of  $\alpha,\beta$ -unsaturated aldehydes to allylic alcohols ( $\text{NiIn}$ ,<sup>17</sup>  $\text{Ni}_3\text{Sn}$ ,<sup>18</sup>  $\text{RuTi}$ <sup>19</sup>), and that of nitrostyrenes to aminostyrenes ( $\text{Pd}_{13}\text{Pb}_9$ ,  $\text{RhPb}_2$ ).<sup>20</sup> It is expected that secondary H addition is inhibited effectively in such a geometrically constrained environment (Scheme 1). Herein, we report efficient catalytic systems for *trans*-ST synthesis from DPA by using intermetallic compounds.

Initially, we examined the suitability of metal elements for *trans*-ST synthesis from DPA as an active component of intermetallic compounds. The catalytic performances of several monometallic catalysts supported on silica ( $\text{M}/\text{SiO}_2$ ;  $\text{M} = \text{Pt}$ ,  $\text{Pd}$ ,  $\text{Rh}$ ,  $\text{Ru}$ , and  $\text{Ni}$ ) were tested in the hydrogenation of DPA in a batch system (Table 1).

**Table 1. Catalytic Performances of Monometallic Catalysts in Hydrogenation of DPA<sup>a</sup>**

M/SiO <sub>2</sub>	time/min	DPA conv. (%)	selectivity (%)		
			<i>trans</i> -ST	<i>cis</i> -ST	DPE
Pt/SiO <sub>2</sub>	60	75	7	77	16
	90	99	7	70	23
Pd/SiO <sub>2</sub>	60	95	3	82	15
	90	99	13	47	40
Rh/SiO <sub>2</sub>	60	63	13	47	40
	90	99	19	22	59
Ru/SiO <sub>2</sub>	60	3.3	10	60	30
Ni/SiO <sub>2</sub>	60	13	3	80	17

<sup>a</sup>Reaction condition: catalyst, 100 mg (metal loading, 3 wt %); DPA, 5.6 mmol; solvent, 7 mL (THF); temperature, 298 K, gas phase, flowing H<sub>2</sub> (20 mL·min<sup>-1</sup>).

Although Pt/SiO<sub>2</sub> and Pd/SiO<sub>2</sub> exhibited high DPA conversions after 60 min, selectivities to *trans*-ST were low. Elongation of the reaction time (90 min) did not increase the selectivity because overhydrogenation to DPE occurred. Ru/SiO<sub>2</sub> and Ni/SiO<sub>2</sub> showed much lower DPA conversions than Pd or Pt catalysts and poor selectivities to *trans*-ST. In contrast, Rh/SiO<sub>2</sub> gave a DPA conversion comparable to that for Pt/SiO<sub>2</sub> and the highest *trans*-ST selectivity. The selectivity at complete conversion was much higher than those of Pt/SiO<sub>2</sub> and Pd/SiO<sub>2</sub>. Thus, Rh had an intrinsic suitability for *trans*-ST synthesis from DPA compared to other metals. This is probably due to its hydrogenation ability being milder than those of Pt and Pd but sufficient to catalyze the semihydrogenation of DPA. The strong hydrogenation ability of Pd comparable to Pt may be related to the easiness of  $\beta$ -PdH<sub>x</sub> formation, which is active for overhydrogenation.<sup>21</sup> We subsequently prepared a series of Rh-based intermetallic compound catalysts (Rh–M′/SiO<sub>2</sub>; M′ = Bi, Ge, In, Sb, and Sn) by successive impregnation with Rh/SiO<sub>2</sub> (see Supporting Information for detailed experimental procedures). Figure 1 shows XRD patterns of the prepared Rh-based catalysts. Monometallic Rh catalyst exhibited broad peaks characteristic to 111 and 200 diffractions of fcc Rh at 41.0° and 47.2°, respectively. RhIn/SiO<sub>2</sub> exclusively generated a peak assigned to a 111 diffraction of RhIn with B2

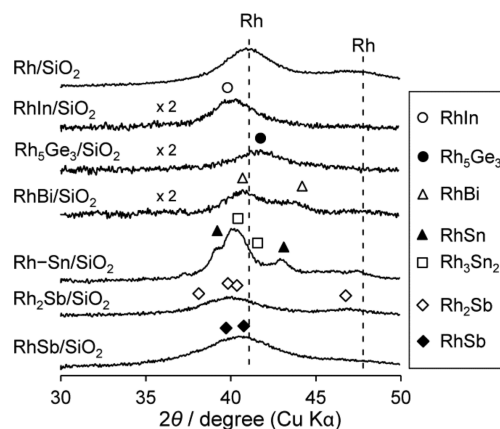


**Figure 1.** XRD patterns of Rh-based catalysts.

structure (space group:  $Pm\bar{3}m$ ), indicating the formation of RhIn intermetallic nanoparticles in single phase. Similar results were also obtained with other bimetallic Rh catalysts, with the exception of Rh–Sn. In the case of Rh–Sn/SiO<sub>2</sub>, a Rh<sub>3</sub>Sn<sub>2</sub> phase was also observed in addition to the RhSn phase.

Crystallite sizes of the intermetallic nanoparticles estimated using the Scherrer's equation on the most intense peaks were 2–4 nm. In the case of RhSb, the peaks were broad and their positions were close to that of monometallic Rh, making the assignment unclear. Although elongation of the H<sub>2</sub> reduction time made the diffraction peaks more clearly to be reasonably assigned to RhSb phase (Figure S1), this resulted in a significant sintering of the particle. TEM observations combined with nanobeam diffraction (NBD) and energy-dispersive X-ray (EDX) analysis were therefore performed for further characterization of RhSb/SiO<sub>2</sub>. As shown in Figure 2, the particle size was 2–3 nm, consistent with the crystallite size.

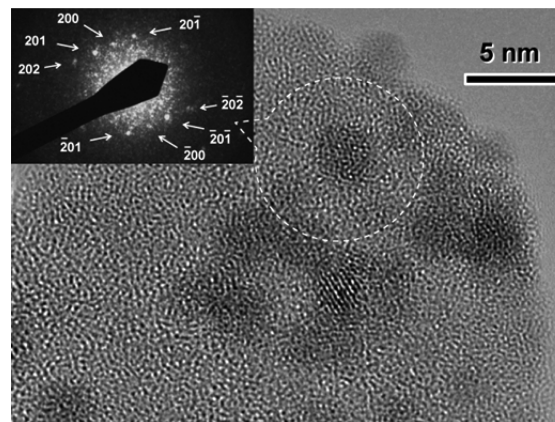


**Figure 2.** TEM image and NBD pattern (inset) of RhSb/SiO<sub>2</sub>. The NBD pattern was acquired at the region designated by the white dotted circle.

Moreover, the NBD pattern focused on a single nanoparticle showed diffraction spots assigned to orthorhombic RhSb (space group:  $Pnma$ ), confirming that the nanoparticles were truly intermetallic RhSb. Lattice fringes with  $d = 2.88 \text{ \AA}$  corresponding to the  $d$ -spacing of RhSb {111} was observed in a HR-TEM image of RhSb/SiO<sub>2</sub> (Figure S2). Moreover, an EDX analysis confirmed that the Rh/Sb atomic ratio of the nanoparticle was 1:1. These results also support the successful formation of intermetallic RhSb nanoparticles. Although the

formation of RhSb was thus confirmed, we cannot completely exclude the presence of small Rh clusters that are hardly observable by XRD.

We investigated the catalytic performances of Rh-based catalysts in the hydrogenation of DPA. Figure 3 shows the

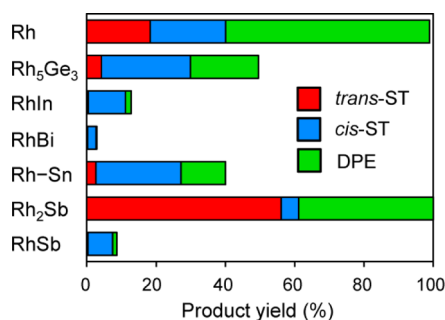


**Figure 3.** Product yields in the hydrogenation of DPA over various Rh-based catalysts. Reaction condition was identical to that in Table 1 footnote.

product yield after 90 min of reaction. Most intermetallic compounds exhibited lower DPA conversions and *trans*-ST yields than Rh/SiO<sub>2</sub>. In contrast, Rh<sub>2</sub>Sb/SiO<sub>2</sub> exhibited a complete conversion of DPA with much higher selectivity to *trans*-ST than Rh/SiO<sub>2</sub>. The time course of the product yields with Rh<sub>2</sub>Sb/SiO<sub>2</sub> is shown in Figure 4.

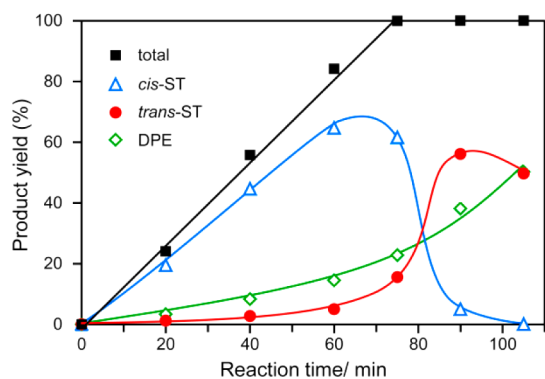


**Figure 4.** Time course of product yield in the hydrogenation of DPA over Rh<sub>2</sub>Sb/SiO<sub>2</sub>.

Semihydrogenation of DPA to *cis*-ST dominantly proceeded until 60 min. After the complete conversion of DPA, the *cis*-ST yield significantly decreased, whereas those of *trans*-ST and DPE increased. This result indicates that isomerization of *cis*-ST to *trans*-ST and overhydrogenation to DPE occurred and that these two reactions were slower than the semihydrogenation of DPA to *cis*-ST. The *trans*-ST yield finally decreased because of the overhydrogenation to DPE (105 min). Consequently, we obtained a maximum yield of *trans*-ST (56%) at 90 min. We should emphasize that this is the first example of preferential synthesis of *trans*- or (*E*)-alkene from an alkyne using a heterogeneous metallic catalyst. Comparing the DPA conversion in terms of Rh fraction ( $m/m + n$  of Rh<sub>*m*</sub>M'<sub>*n*</sub>/SiO<sub>2</sub>), it was observed that Rh-based catalysts containing intermetallic phases with Rh fractions higher than 0.5 (Rh<sub>2</sub>Sb, 0.667 > Rh<sub>5</sub>Ge<sub>3</sub>, 0.625 > Rh<sub>3</sub>Sn<sub>2</sub>, 0.600) exhibited high or moderate conversion.

In general, the formation of an intermetallic phase results in the dilution of Rh–Rh sites on the catalyst surface. Therefore, a higher Rh fraction retains more Rh–Rh sites, which are necessary for dissociative adsorption of H<sub>2</sub>. Although dissociative adsorption of H<sub>2</sub> is mandatory for semihydrogenation of DPA, an excess capability of H<sub>2</sub> activation causes undesired overhydrogenation to DPE. Therefore, the highest *trans*-ST yield obtained with Rh<sub>2</sub>Sb may be due to its moderate hydrogenation ability. Conversely, RhBi, RhIn, and RhSb exhibited low DPA conversions with almost no production of *trans*-ST. This can be attributed to their poor hydrogenation abilities.

We subsequently performed similar reactions using *cis*-ST as a reactant to clarify the catalytic performances of these Rh-based intermetallic compounds in the isomerization of *cis*-ST to *trans*-ST. Table 2 summarizes the results after 200 min of the reaction.

**Table 2.** Catalytic Performances of Rh-Based Intermetallic Catalysts in the Isomerization of *cis*-ST<sup>a</sup>

Rh <sub><i>m</i></sub> M' <sub><i>n</i></sub> /SiO <sub>2</sub>	<i>cis</i> -ST conv. (%)	selectivity (%)	
		<i>trans</i> -ST	DPE
Rh <sub>5</sub> Ge <sub>3</sub> /SiO <sub>2</sub>	63	64	36
RhIn/SiO <sub>2</sub>	3.3	66	34
RhBi/SiO <sub>2</sub>	0.4	81	19
Rh–Sn/SiO <sub>2</sub>	2.7	59	41
Rh <sub>2</sub> Sb/SiO <sub>2</sub>	89	70	30
RhSb/SiO <sub>2</sub>	35	93	7.0

<sup>a</sup>Reaction condition is identical to that in Table 1, except with a reaction time of 200 min.

Rh<sub>5</sub>Ge<sub>3</sub> and Rh<sub>2</sub>Sb showed high *cis*-ST conversions with moderate *trans*-ST selectivities, a result similar to that using DPA. RhSb exhibited a moderate conversion (35%) and high selectivity (93%). Other catalysts gave very low conversions. Thus, it was revealed that the hydrogenation ability was significantly affected by not only the difference in the Rh fraction but also that in the second metal. The effect of Sb content on the catalytic property was then investigated. A volcano relationship was observed between reaction rate and Sb content with ca. 0.1 of Sb content at the top (Figure S3). A possible interpretation is competition of a positive ligand effect of Sb modifying the electronic state of Rh and a negative ensemble effect of Sb reducing the number of Rh–Rh sites. In contrast to the catalytic activity, the selectivity increased monotonically with the increase in Sb content (Figure S3). The effect of H<sub>2</sub> pressure ( $P_{H_2}$ ) on the reaction outcome with RhSb/SiO<sub>2</sub> was also investigated. A kinetic study revealed that both reaction rate and selectivity to *trans*-ST were almost independent of  $P_{H_2}$  (Figure S4).

Figure 5 shows conversion–selectivity curves in the isomerization of *cis*-ST. To obtain high conversions, the reaction over RhSb was also performed at 333 K. For Rh and Rh<sub>2</sub>Sb, the selectivities declined slightly at high conversion levels. In contrast, RhSb retained high selectivity even at 97% conversion, which afforded a 94% yield of *trans*-ST. This is the first report of a highly selective isomerization of *cis*-alkene to *trans*-alkene over a metallic catalyst. The small deviation from 100% selectivity may be due to the presence of a trace amount of monometallic Rh clusters. Thus, the RhSb catalyst possesses a unique catalytic property: hydrogenation of DPA and ST was

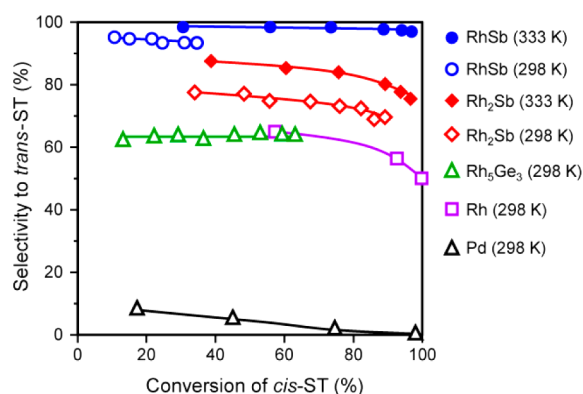


**Figure 5.** Conversion–selectivity curves in the isomerization of *cis*-ST to *trans*-ST for various catalysts.

hardly catalyzed, whereas isomerization of *cis*-ST occurred effectively. This trend can be attributed to a specific hydrogenation ability of RhSb, capable of half-hydrogenation but minimal overhydrogenation, as described in Scheme 1. With regard to the reaction at 333 K, higher selectivities were obtained than that at 298 K. This result suggests that not only were formation rates of *trans*-ST enhanced but overhydrogenation was also well-inhibited even at 333 K.

The results obtained above led us to an idea of a tandem catalytic system effective for *trans*-ST synthesis from DPA using selective catalysts for semihydrogenation of DPA to *cis*-ST and the subsequent isomerization to *trans*-ST. As mentioned above, we have reported that Pd<sub>3</sub>Bi/SiO<sub>2</sub> selectively catalyzed semihydrogenation of DPA to *cis*-ST.<sup>11</sup> Therefore, a combination of Pd<sub>3</sub>Bi/SiO<sub>2</sub> and RhSb/SiO<sub>2</sub> is expected to effectively produce *trans*-ST from DPA. Figure 6 shows the time courses

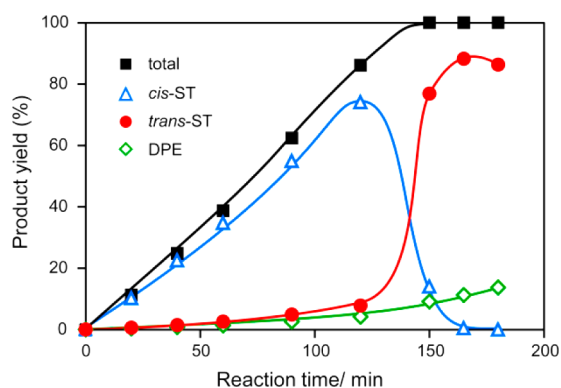


**Figure 6.** Time course of product yields in the hydrogenation of DPA using Pd<sub>3</sub>Bi/SiO<sub>2</sub> and RhSb/SiO<sub>2</sub>. Reaction condition was identical to that in Table 1 footnote, with the exception of the catalyst amount (Pd<sub>3</sub>Bi/SiO<sub>2</sub>, 100 mg; RhSb/SiO<sub>2</sub>, 200 mg) and temperature (333 K).

of product yields in the hydrogenation of DPA using Pd<sub>3</sub>Bi/SiO<sub>2</sub> and RhSb/SiO<sub>2</sub>. At the initial stage of the reaction (~90 min), *cis*-ST was predominantly obtained, suggesting that semihydrogenation of DPA to *cis*-ST over Pd<sub>3</sub>Bi/SiO<sub>2</sub> proceeded. This was confirmed by hydrogenation of DPA over RhSb/SiO<sub>2</sub> alone at 333 K, which showed much lower *cis*-ST yield (Figure S5).

After an 80% conversion of DPA, *trans*-ST yield drastically increased with a steep drop in the *cis*-ST yield, indicating isomerization of *cis*-ST to *trans*-ST over RhSb/SiO<sub>2</sub>. Finally, the *trans*-ST yield reached 88% at 165 min. Elongation of the

reaction time resulted in a slight decline in the *trans*-ST yield. Thus, as expected, *trans*-ST synthesis from DPA was successfully achieved using the tandem catalytic system with Pd<sub>3</sub>Bi/SiO<sub>2</sub> and RhSb/SiO<sub>2</sub>.

In conclusion, we developed novel catalytic systems based on intermetallic compounds effective for *trans*-ST synthesis from DPA. Rh<sub>2</sub>Sb/SiO<sub>2</sub> catalyzes both the semihydrogenation of DPA to *cis*-ST and the subsequent isomerization to *trans*-ST, affording a moderate *trans*-ST yield (58%). RhSb/SiO<sub>2</sub> possesses a unique hydrogenation property capable of half-hydrogenation but minimal overhydrogenation, which enables selective isomerization of *cis*-ST to *trans*-ST. A tandem catalytic system with Pd<sub>3</sub>Bi/SiO<sub>2</sub> and RhSb/SiO<sub>2</sub> effectively produces *trans*-ST from DPA. The observed unique catalysis seems to be originated from the specific atomic arrangements of the intermetallic compound surfaces. As is the case of the selective hydrogenation catalysts ever reported,<sup>21–23</sup> quantum chemical calculations with specific surface atomic arrangements of RhSb will provide a strong suggestion for the unique catalysis of RhSb. Thus, the obtained insights in this study not only provide an efficient catalytic system for *trans*-ST synthesis but also open up a new field of heterogeneous catalysis, i.e., stereoselective chemical transformation controlled by a highly ordered bimetallic surface.

## ■ ASSOCIATED CONTENT

### Supporting Information

Experimental details, XRD patterns, HR-TEM images, and other reaction data. This material is available free of charge via the Internet at <http://pubs.acs.org>.

## ■ AUTHOR INFORMATION

### Corresponding Author

\*E-mail: [komatsu.t.ad@m.titech.ac.jp](mailto:komatsu.t.ad@m.titech.ac.jp). Fax: +81-3-5734-2758. Tel.: +81-3-5734-3532.

### Notes

The authors declare no competing financial interest.

## ■ ACKNOWLEDGMENTS

This work was supported by JSPS KAKENHI Grant No. 23360353. We thank Center for Advanced Materials Analysis Tokyo Institute of Technology for the aid of TEM observation.

## ■ REFERENCES

- (1) Wong-Wah-Chung, P.; Mailhot, G.; Bolte, M. *J. Photochem. Photobiol., A* **2001**, *138*, 275–280.
- (2) Ichimura, K. *Chem. Rev.* **2000**, *100*, 1847–1873.
- (3) Halim, M.; Samuel, I. D. W.; Pillow, J. N. G.; Monkman, A. P.; Burn, P. L. *Synth. Met.* **1999**, *102*, 1571–1574.
- (4) McNulty, J.; Das, P. *Eur. J. Org. Chem.* **2009**, 4031–4035.
- (5) Beletskaya, I. P.; Cheprakov, A. V. *Chem. Rev.* **2000**, *100*, 3009–3066.
- (6) Lindlar, H. *Helv. Chim. Acta* **1952**, *35*, 446–456.
- (7) Guzzi, L.; Schay, Z.; Stefler, G.; Liotta, L. F.; Deganello, G.; Venezia, A. M. *J. Catal.* **1999**, *182*, 456–462.
- (8) Zhang, Q. W.; Li, J.; Liu, X. X.; Zhu, Q. M. *Appl. Catal., A* **2000**, *197*, 221–228.
- (9) Armbruster, M.; Kovnir, K.; Behrens, M.; Teschner, D.; Grin, Y.; Schlogl, R. *J. Am. Chem. Soc.* **2010**, *132*, 14745–14747.
- (10) Ota, A.; Armbruster, M.; Behrens, M.; Rosenthal, D.; Friedrich, M.; Kasatkin, I.; Girgsdies, F.; Zhang, W.; Wagner, R.; Schlogl, R. *J. Phys. Chem. C* **2011**, *115*, 1368–1374.
- (11) Komatsu, T.; Takagi, K.; Ozawa, K. *Catal. Today* **2011**, *164*, 143–147.

- (12) Vile, G.; Almora-Barrios, N.; Mitchell, S.; Lopez, N.; Perez-Ramirez, J. *Chem.—Eur. J.* **2014**, *20*, 5926–5937.
- (13) Michaelides, I. N.; Dixon, D. J. *Angew. Chem., Int. Ed.* **2013**, *52*, 806–808.
- (14) Armbruster, M.; Kovnir, K.; Friedrich, M.; Teschner, D.; Wowsnick, G.; Hahne, M.; Gille, P.; Szentmiklosi, L.; Feuerbacher, M.; Heggen, M.; Girgsdies, F.; Rosenthal, D.; Schlogl, R.; Grin, Y. *Nat. Mater.* **2012**, *11*, 690–693.
- (15) Li, C. M.; Chen, Y. D.; Zhang, S. T.; Zhou, J. Y.; Wang, F.; He, S.; Wei, M.; Evans, D. G.; Duan, X. *ChemCatChem* **2014**, *6*, 824–831.
- (16) Armbruster, M.; Wowsnick, G.; Friedrich, M.; Heggen, M.; Cardoso-Gil, R. *J. Am. Chem. Soc.* **2011**, *133*, 9112–9118.
- (17) Li, C. M.; Chen, Y. D.; Zhang, S. T.; Xu, S. M.; Zhou, J. Y.; Wang, F.; Wei, M.; Evans, D. G.; Duan, X. *Chem. Mater.* **2013**, *25*, 3888–3896.
- (18) Rodiansono; Khairi, S.; Hara, T.; Ichikuni, N.; Shimazu, S. *Catal. Sci. Technol.* **2012**, *2*, 2139–2145.
- (19) Ruiz-Martinez, J.; Fukui, Y.; Komatsu, T.; Sepulveda-Escribano, A. *J. Catal.* **2008**, *260*, 150–156.
- (20) Furukawa, S.; Yoshida, Y.; Komatsu, T. *ACS Catal.* **2014**, *4*, 1441–1450.
- (21) Lopez, N.; Vargas-Fuentes, C. *Chem. Commun.* **2012**, *48*, 1379–1391.
- (22) Delbecq, F.; Sautet, P. *J. Catal.* **2003**, *220*, 115–126.
- (23) Krajci, M.; Hafner, J. *J. Catal.* **2012**, *295*, 70–80.